

BINP STATUS REPORT

I. A. Koop
Budker Institute of Nuclear Physics,
Novosibirsk, 630090, Russia

Abstract

In this report the overview of activity at existing and developed electron-positron high energy colliders at BINP is presented. The operating machines are the VEPP-4M storage ring being running now at J/Psi and the VEPP-5 preinjector linac. The VEPP-2000 collider, which is under construction, will operate with round beams at the energy of up to 1 GeV per bunch. Current results and future plans are discussed.

1 VEPP-4M COLLIDER

VEPP-4M is a single-ring e+e- collider now operated for the high-energy physics experiments, photo-nuclear study at ROKK-1M facility and synchrotron radiation researches [1, 2]. Maximum designed energy of VEPP-4M is around 6 GeV. Electron (or positron) beam consists of two bunches, which are spaced by one-half of the ring circumference (183 m). Beams collide at zero crossing angle in the interaction point (IP), where the KEDR detector is located.

Basically, VEPP-4M is intended to study physics of Υ - meson and two-photon processes. However, because of the interest growing to the range of J/ψ and ψ' physics, it was proposed to concentrate efforts in the low energy range $E = 1.5 - 1.8$ GeV [3]. This energy range is unusual for such high energy storage ring and additional investigations have to be done to obtain optimal performance.

Two possible ways to reach reasonable luminosity in J/ψ region are under consideration: (i) redistribution of the damping partition numbers with the help of the gradient wigglers (GWs) installed in the technical straight at places with non zero dispersion and (ii) introducing of a strong radiation damping by two 3-pole dipole wigglers (DWs) located on the opposite sides of the VEPP-4M experimental straight section.

In the near future is planned to perform an experiment on the measurement of the τ -lepton mass in vicinity of its production threshold (1.777 GeV) with the relative accuracy better than 10^{-4} using the resonance depolarization technic for a beam energy calibration [4]. Earlier, such a method was successfully used in measurements of the J/ψ and ψ' mass at VEPP-4 [5].

1.1 Luminosity

For VEPP-4 the peak luminosity at 5 GeV was about $5 \cdot 10^{30} \text{ cm}^{-2} \text{ s}^{-1}$. Now for VEPP-4M at the same energy we hope to reach $2 \cdot 10^{31} \text{ cm}^{-2} \text{ s}^{-1}$ with the existing optics. At low energy the luminosity reduces significantly ($\propto E^4$) and

different problems arise due to low damping rates ($1/\tau \sim 10 \text{ s}^{-1}$).

VEPP-4M has a relatively large horizontal dispersion at the IP, so the horizontal beam size there is mainly defined by the energy spread. The ratio between synchrotron and betatron horizontal beam sizes is equal to $\lambda = 1.8$ in the nominal operation mode. However, at low energy we can vary this parameter by the GWs, which can redistribute damping decrements between horizontal and longitudinal planes. By changing of the GWs strength and VEPP-4M lattice, we can vary λ within rather wide range (from ~ 1 to 4). Analytical studies [6] shows, that the beam-beam effects are most dangerous for $\lambda = 1$. In this case all three degrees of freedom are coupled and synchro-betatron resonances become strong.

On the contrary, when $\lambda \gg 1$, the particle horizontal co-ordinate at the IP practically does not depend on the betatron motion and the beam behaviour becomes almost two-dimensional. The width of the horizontal and coupled synchro-betatron resonances falls down with increasing of λ (for the pure vertical and synchrotron resonances it is not the case). Experimental results show that for $\lambda \approx 3$ the maximum bunch current obtained is around 2 mA, that corresponds to $\xi_x \approx 0.02$. For the nominal operation mode ($\lambda \approx 1.8$) such a current can not be reached because in this case $\xi_x = 0.032$ is well above the beam-beam limit.

Fig.1 shows the luminosity obtained during summer 2001 run, while Fig.2 depicts the vertical beam-beam parameter as a function of the bunch current. The maximum peak luminosity that was achieved $L = 4.7 \cdot 10^{29} \text{ cm}^{-2} \text{ s}^{-1}$ corresponds to $\xi_y = 0.037$ (1×1 bunch mode with 2.2 mA per bunch).

Another way to improve the luminosity performance is using of dipole wigglers (DWs) with the peak field $H = 1.8$ T, which allows one to increase the horizontal emittance by a factor of 4 at 1.5 GeV. Numerical simulations of the beam-beam interaction with the LIFETRACK code [7] show that with the help of the DWs we can reach the single bunch luminosity $L \approx 10^{30} \text{ cm}^{-2} \text{ s}^{-1}$ for 1.5 GeV (with beam-beam parameters $\xi_x = 0.015$ and $\xi_y = 0.03$). The experimental data with the switched-on DWs correspond to $L \approx 0.7 \cdot 10^{30} \text{ cm}^{-2} \text{ s}^{-1}$ ($I_b = 3.2$ mA, $\xi_y = 0.046$) and the beam lifetime $\tau = 1.3$ hour. Experiments show that the maximum emittance increase due to DWs (4 times) is not optimal for obtaining of high luminosity. The reason is, as it is considered below, the dynamic aperture limitation.

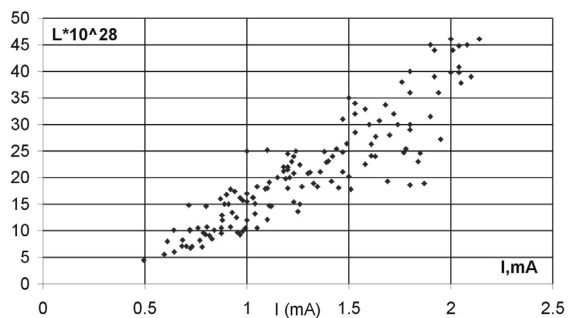


Figure 1: Single bunch luminosity versus the beam current (Dipole Wigglers off).

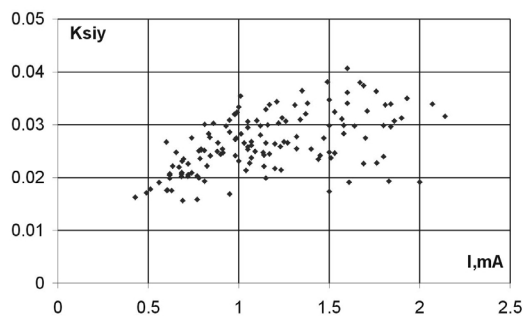


Figure 2: Vertical beam-beam parameter calculated from luminosity data taken in the test run.

1.2 Dynamic aperture

Study of the non-linear beam dynamics was already performed at VEPP-4M several years ago [8]. Since that time, the new final focus quadrupoles with the improved gradient quality replaced two old ones. Besides, the working betatron tune point was moved from (8.62, 7.57) to (8.55, 7.60). These two factors yielded to significant increase of the horizontal border of stable motion (about twice). However, when two dipole wigglers are used to enlarge the beam phase volume, the horizontal aperture shrinks. At the energy of 1.5 GeV, two 1.8 T dipole wigglers provide strong distortions to the beam motion (especially vertical). At their maximum field the linear tune shift is $\Delta Q_y \approx 0.13$ and $\Delta Q_x \approx 0.02$ [9].

Linear wiggler effects, including the tune matching and the beta-function recovering (inside a 15% accuracy), are completed by three pairs of quadrupoles in the experimental straight section. However, non-linear components of the wiggler field (mainly, strong sextupole components) together with the fringe field's yield a significant reduction

of the dynamic aperture (by approximately 30%) as it is illustrated in Fig.3 [10]. The vertical border of the aperture is limited by mechanical factors well below the dynamic aperture limitation and is not changed due to the wigglers switching-on.

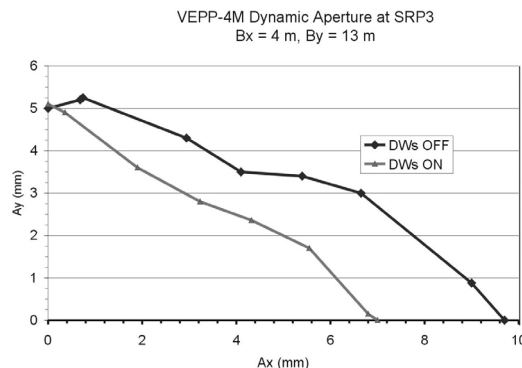


Figure 3: VEPP-4M dynamic aperture.

As the next step, study of non-linear components of the wiggler field is planning to be performed. The final goal is suppression of the DWs non-linearity by using of octupole and sextupole magnets.

1.3 Polarization

A measurement of the $\tau^+\tau^-$ production cross section will be done by the detector KEDR in the energy region just above the threshold (1.78 GeV). To calibrate the beam energy, the polarized electron beam is injected in the storage ring VEPP-4M from a booster storage ring VEPP-3 (see Fig.4). Radiative selfpolarization of particles in VEPP-3 occurs with the characteristic time $\tau_p \approx 40$ minutes near to the τ threshold (for VEPP-4M $\tau_p \approx 85$ hours).

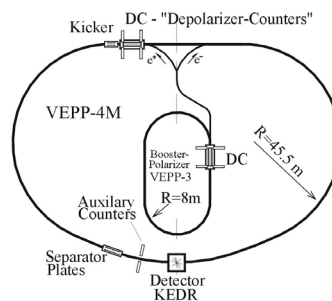


Figure 4: A set up for the polarization experiments at VEPP-4M.

Quantum fluctuations of the synchrotron radiation together with imperfections of the magnetic field depolarizes a beam with the characteristic spin relaxation time τ_T .

We believe the horizontal magnetic field produced by vertically misaligned quadrupole magnets is a main factor of depolarization. Estimations show that for the τ threshold energy of 1777 MeV and for the vertical closed orbit distortions of $\sim 100\mu m$ (rms), the polarization decay time for VEPP-4M is equal to $\tau_r \approx 30$ minutes [4]. The depolarization rate depends strongly on the spin resonance tune: $\tau_p\tau_r \propto (\nu_s - k)^{-4}$ (at $E = 1777$ MeV we have $\nu_s = 4.032$). This fact can limit the energy calibration run time.

Experimental set up for the depolarization study at VEPP-4M includes 4 movable scintillation counters inserted into the vacuum tube and 2 strip-line electrodes to produce the resonant spin depolarization. The counters detect the Touschek scattering electrons, whose scattering rate depends on the particle spin. One bunch of polarized particles and one bunch of unpolarized particles are used simultaneously to measure the ratio $1 - N_2/N_1$ depending on the depolarizer signal frequency, where N_1 and N_2 are counts for the first and the second bunch.

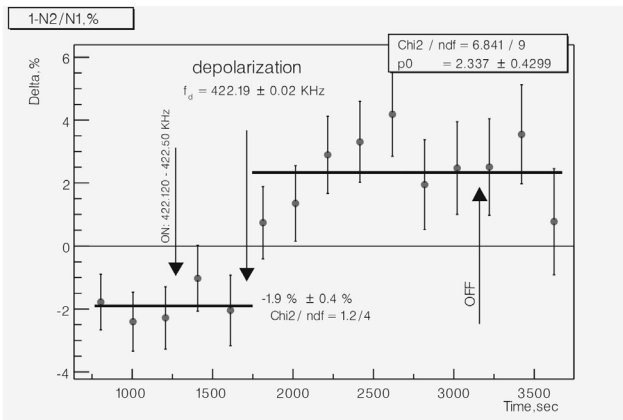


Figure 5: Test run on energy calibration at VEPP-4M.

To study the method and to check the KEDR detector data acquisition system, a J/ψ test run was performed in summer 2001. Fig.5 shows typical "jump" in $1 - N_2/N_1$ due to the beam depolarization. The error of the beam energy definition obtained during the test run is ≈ 30 keV ($\Delta E/E \approx 2 \cdot 10^{-5}$).

1.4 Future plans

- Commissioning of the new polarimeter system at the VEPP-4M.
- Measurement of the beam energy by the method of resonance depolarization with reasonable accuracy ($\Delta E/E \approx 1 \times 10^{-5}$) in the energy range between J/ψ and τ .
- The KEDR run at J/ψ peak and in the vicinity of the threshold of τ -lepton production.

2 VEPP-2000 COLLIDER

Since the end of 1992 the e^+e^- collider VEPP-2M in Novosibirsk has been successfully running in the c.m. energy range from threshold of hadron production up to 1.4 GeV. Since 1984 VEPP-2M is operating with the five poles superconducting wiggler with the maximum field $B = 8$ T, which increases the beam emittance by a factor of ≈ 3 . The integrated luminosity of about 50 pb^{-1} was collected with two modern detectors SND [11] and CMD-2 [12] allowing precise measurements of most of the hadronic channels of e^+e^- annihilation. Together with 24 pb^{-1} collected at VEPP-2M in the previous generation of experiments in 1974-1987, this integrated luminosity is more than one order of magnitude higher than about 6 pb^{-1} accumulated by various experimental groups in Frascati and Orsay in the c.m. energy range from 1.4 to 2 GeV. Thus, there is a serious energy gap between the maximum energy attainable at VEPP-2M and 2 GeV in which existing data on e^+e^- annihilation into hadrons are rather imprecise. Accurate measurements of hadronic cross sections in this energy range are crucial for better understanding of many phenomena in high energy physics.

A recent decision to upgrade the VEPP-2M complex by replacing the existing collider with a new one, in order to improve the luminosity and at the same time increase the maximum attainable energy up to 2 GeV, will significantly broaden the potential of experiments performed at the collider. Following modern trends, the new project was named VEPP-2000 (see the Fig. 6).

2.1 Round Colliding Beams Concept

The basic parameter of a collider is its luminosity L which in the case of short bunches is determined by the formula:

$$L = \frac{\pi\gamma^2\xi_z\xi_x\epsilon_x f}{r_e^2\beta_z} \cdot \left(1 + \frac{\sigma_z}{\sigma_x}\right)^2,$$

where ξ_z, ξ_x are the space charge parameters whose maximum values are limited by the beam-beam effects; ϵ_x is the horizontal emittance of the beams, σ_z, σ_x are their r.m.s. sizes at the interaction point (IP), and β_z is the vertical β -function at the IP; f is the frequency of collisions at this IP, r_e is the classical electron radius, γ is the relativistic factor.

The space charge parameter per interaction is:

$$\xi_{x,z} = \frac{Nr_e}{2\pi\gamma} \frac{\beta_{x,z}}{(\sigma_x + \sigma_z)\sigma_{x,z}},$$

where N is the number of particles in the opposite bunch. Colliding bunches with maximum values of $\xi_z \approx 0.05$ and $\xi_x \approx 0.02$ are experimentally obtained on the VEPP-2M collider[13].

Aiming at a very high luminosity due to raising the ξ limits in the Novosibirsk Φ -Factory project[14, 15], colliding beams with round transverse cross-sections were proposed (just "round beams" in what follows). During the last decade at BINP, this approach evolved into the concept of Round Colliding Beams (RCB)[16].

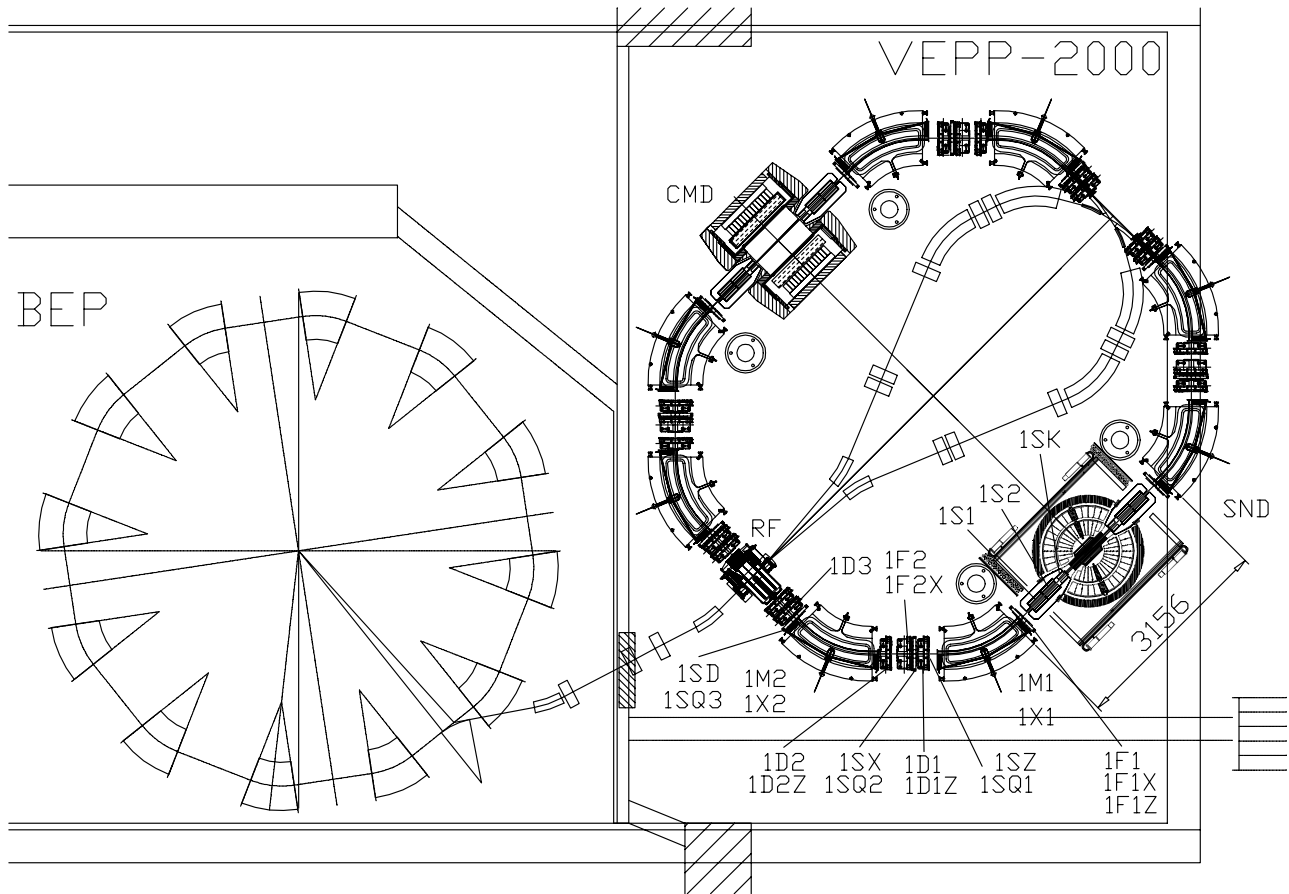


Figure 6: The VEPP-2000 collider layout

In the RCB case, the luminosity formula has the form:

$$L = \frac{4\pi\gamma^2\xi^2\epsilon f}{r_e^2\beta}$$

and the space charge parameters are now the same in the two directions, so the horizontal parameter can be strongly enhanced.

The evident advantage of round colliding beams is that with the fixed particle density, the tune shift from the opposite bunch becomes twice as small as the tune shift in the case of flat colliding beams. Besides, the linear beam-beam tunes shift in the round beams becomes independent of the longitudinal position in the bunch, thereby weakening the action of synchro-betatron resonances.

The main feature of the RCB is rotational symmetry of the kick from the round opposite beam; complemented with the $X - Z$ symmetry of the betatron transfer matrix between the collisions, it results in an additional integral of motion $M = xz' - zx'$, i.e. the longitudinal component of particle's angular momentum is conserved. Thus, the transverse motion becomes equivalent to a one-dimensional (1D) motion. Resulting elimination of all betatron coupling resonances is of crucial importance, since they are believed to cause the beam lifetime degradation

and blow-up.

The above arguments in favour of RCB have been checked out by the computer simulations of the beam-beam effects in the VEPP-2M collider lattice, modified to the RCB option[17]. The main results of the simulations[18] are presented in Fig. 7, where the beam sizes are plotted versus the space charge parameter ξ . One can see that the beam blow-up for the round beam option is much weaker than what is simulated by the same code for flat colliding beams (dashed line). The simulations have also demonstrated stability of RCB against the "flip-flop" effect, similarly to conclusions from simple flip-flop models[19].

2.2 Magnets

The lack of space for placing the new machine lead to demand on using of strong dipole magnets. For the energy of particles in the beam to be 1 GeV the field of a magnitude 2.3 T is needed. For this purpose it is planned to use the construction of magnets of booster BEP [20] that works at the level of the magnetic field needed. The parameters of magnets are shown in Table 1.

Construction of magnets with such a big field requires the optimization of coils placement, shape of a pole and

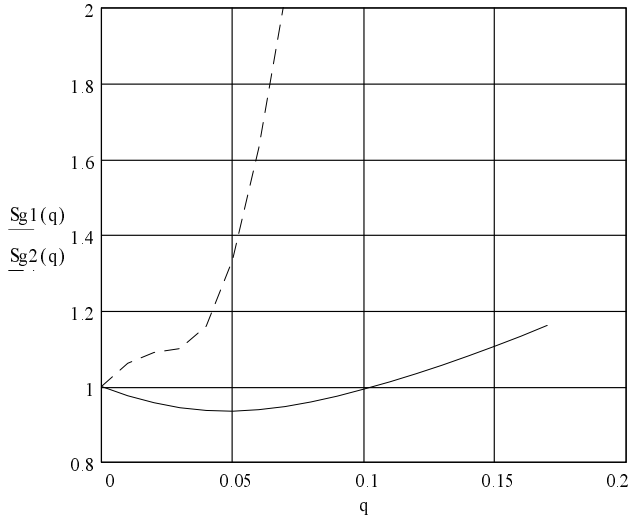


Figure 7: Variation of the weak beam size versus the space charge parameter ξ : solid curve for the round colliding beams, dashed curve for the flat beam option.

Table 1: The main parameters of the bending magnets

Gap	40 mm
Bending angle	45°
Bending radius	1.40 m
Maximal field	2.3 T
Number of coil turns	10
Current in coil	9 kA
Power consumption	900 kW

magnet yoke for decreasing the effect of iron saturation, power consumption and obtaining sufficient region of uniform field. The Fig. 9 shows the guide field distribution versus the longitudinal coordinate at the edge of the dipole magnet. It was obtained by calculations with the *MERMAID* code.

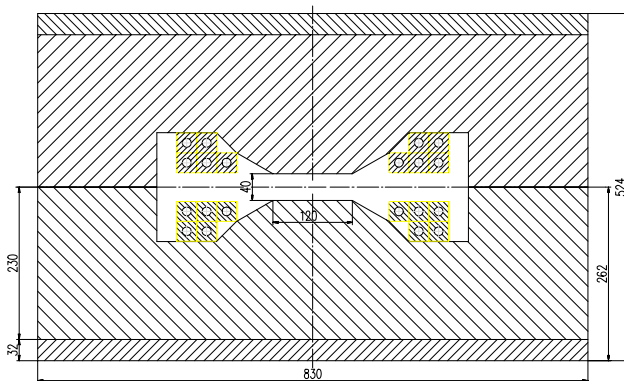


Figure 8: Cross-section of the VEPP-2000 dipole magnet.

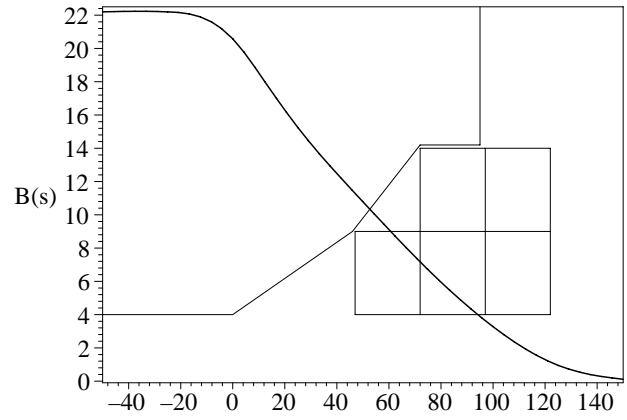


Figure 9: The dependence of the guide field of dipole magnet on the longitudinal coordinate (*MERMAID* data). The edge of a magnet and its coil are shown schematically.

2.3 Solenoids

Focusing in the two interaction regions is performed by SC solenoids, installed symmetrically with respect to the IPs. Each solenoidal block consists of a main solenoid which is longitudinally divided into two parts, and a compensating solenoid with reverse field to adjust longitudinal field integral and focussing. Such a scheme gives an additional possibility to control the β^* value by feeding only one half of the main solenoid at lower energies.

The solenoid coil is divided into three sections: inner section has thickness 30 mm and is made of Nb₃Sn wire 1.23 mm in diameter (50% Cu + 50% Nb₃Sn); middle section has thickness 20 mm and is wound with a NbTi wire 1.2 mm in diameter (48% Cu + 52% NbTi) and outer layer has thickness of 10 mm, made of NbTi wire 0.85 mm in diameter (48% Cu + 52% NbTi). To feed this three-section coil we plan to use two power supply units. Connection scheme implies that the current in the outer section is the sum of currents in the inner ones. The distribution of currents in the sections is: inner section - 145 A, intermediate section - 167 A, outer section - 312 A. The peak magnetic field is 12.1 T.

Table 2: The main parameters of solenoids

Solenoid	Main	Compensating
Magnetic field, T	12.7	9.0
Coil length, m	0.526	0.128
Inductance, H	14.3	1.2
Number of turns	26080	4940
Stored energy, kJ	346	27

Magnetic flux is closed by the iron return yoke located together with all the coils in a common LHe cryostat. Aperture of the coil is 50.0 mm. The inner tube of the helium vessel is a part of the collider vacuum chamber. A liquid nitrogen cooled liner is envisaged to protect the surface of the

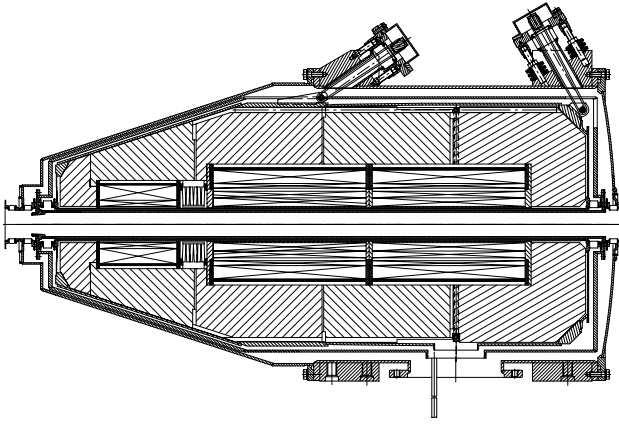


Figure 10: The superconducting solenoid of VEPP-2000

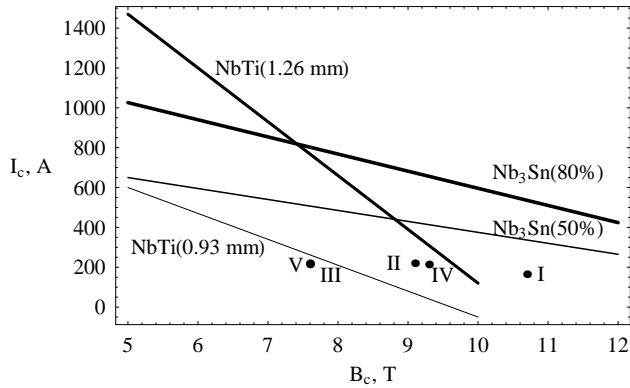


Figure 11: The critical parameters of the superconducting wires used. I — (10.7 T, 165 A), II — (9.1 T, 220 A), III — (7.6 T, 220 A), IV — (9.3 T, 214 A), V — (7.6 T, 214 A)

helium cryostat from heating by the synchrotron radiation.

2.4 RF System

Beam revolution frequency is 12.292 MHz. The accelerating RF frequency was chosen at 14-th revolution frequency harmonic i.e. 172 MHz. With accelerating voltage of 100 kV the bunch length is about $\sigma = 3$ cm at the energy of 1 GeV. Energy loss per turn is 64 keV, and with colliding beam currents of 2×0.1 A the power delivered to the beams is 12.8 kW. The so-called single-mode cavity is proposed to be used to ease suppression of coherent instabilities, see Fig. 12. Two coaxial damping loads are foreseen to absorb the energy from high-order modes excitation. The fundamental mode is isolated from the upper load by the tunable choke.

The RF field distribution of accelerating mode on the axis of the RF cavity is shown in Fig. 13.

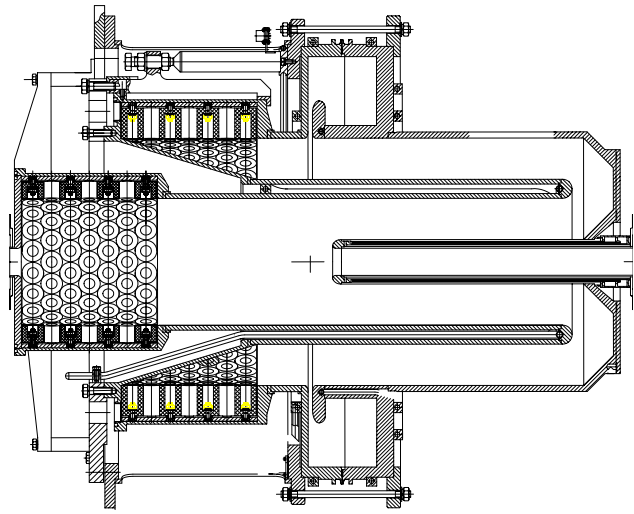


Figure 12: Cross-section of the cavity

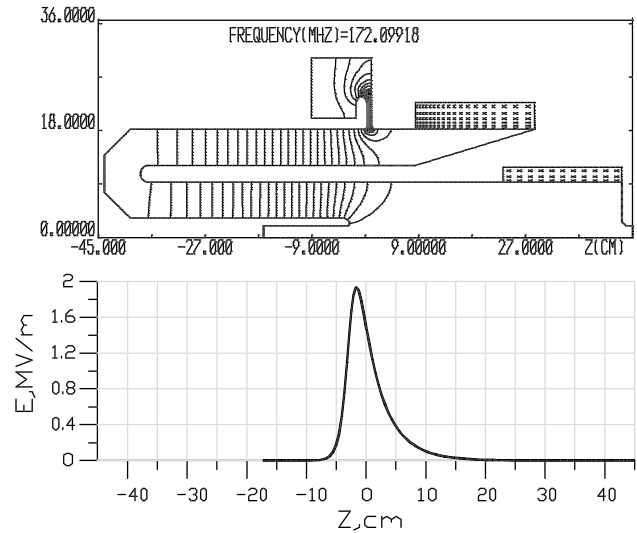


Figure 13: The RF field distribution of the accelerating mode of RF cavity (upper picture). The field distribution on the cavity axis (lower picture)

2.5 Vacuum System

The high-vacuum system consists of 16 ports with ion-getter pumps PVIG-100, which are located at the edges of bending magnets vacuum chambers; of ion-getter pump PVIG-250 connected to the RF cavity; of 4 cryopumps formed of cool solenoid surface. To prevent heating cryosurface, which is under 4.2 K, by SR there is planned to use perforated liner cooled with the liquid nitrogen. The liners ports should provide linear pumping rate of 5 l/s/cm for the nitrogen. The cool surface under 4.2 K is an ideal pumping for all the residual gases but the hydrogen, because after accumulation more than one cryosrpted hydrogen monolayer the saturated vapor pressure of the hydrogen reaches the value of $5 \cdot 10^{-7}$ Torr under given tempera-

ture. In spite of this circumstance our calculations showed that in general the beam life time will depend on residual CO pressure. Numerical simulation of the pressure over the ring was performed under following conditions:

- $I_p = I_e = 200$ mA — electron and positron beam currents
- S_1, S_2, \dots, S_{16} — lumped ports with the pumping rate of 150 l/s, $S_p = 5$ l/s/cm — distributed cryopumping
- Photon flux is $2 \times 2 \cdot 10^{19}$ photon/s/rad
- Coefficient of photostimulated desorption (for after more than 100 Ah):
 - for non-heated chamber sections — 310^{-5} molecule/photon
 - for heated chamber sections — 310^{-6} molecule/photon

The graph of CO pressure distribution for one quarter of the VEPP-2000 circumference and the view on vacuum chamber are shown in the Fig. 14.

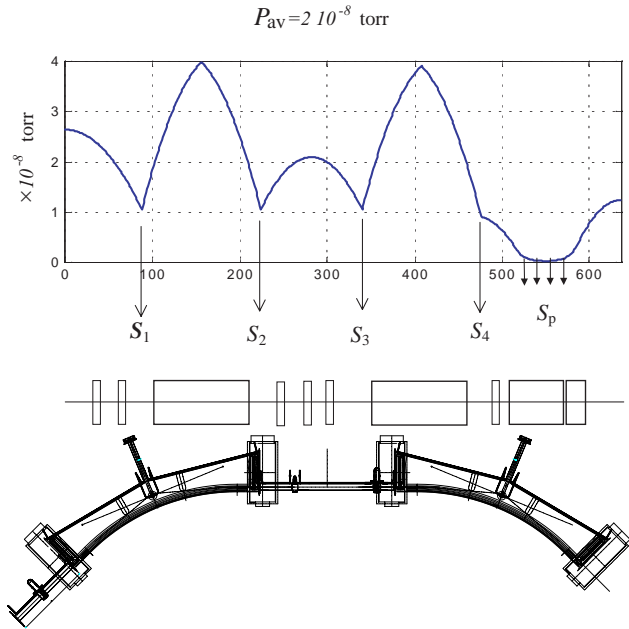


Figure 14: The CO pressure distribution and the vacuum chamber of one quadrant of the VEPP-2000.

2.6 Beam Injection

The injection of beams into the storage ring is planned to be done in the horizontal plane into the long drift opposite to the RF cavity (see the Fig. 6). The inflector plates will be placed on the inner side of the vacuum chamber in the bending magnets at the ends of the drift. The advantage of such a scheme is independence of the injected beam

trajectory on the solenoids field. This gives us an opportunity to test different options of optics: usual round beams, “Möbius”, and flat beams with zero rotation of the betatron oscillation plane.

In Table 3 the main parameters of generators are collected.

Table 3: The main parameters of kickers feed generators

Parameter	Value
charging voltage	up to 40 kV
Polarity of charging voltage	positive
Amplitude of the output pulse	up to 30 kV
Half-height pulse duration	80 ns
Pulse leading/trailing edge duration	60 ns
Output pulse polarity	negative
Output impedance	12,5 Ohm
Each circuite of DSC impedance	6,25 Ohm
Thyratron current amplitude	up to 4,8 kA
Repetition frequency	1 Hz

The BEP booster is capable of production beams with the energy of up to 900 MeV. Thus, operation at lower energies will be continuous, with injection of the beam at the experiment energy. In region from 900 MeV to 1 GeV the energy ramping from 900 MeV to the experiment energy is required.

2.7 VEPP-2000 Parameters

The optical functions of the round beam lattice of VEPP-2000 are presented in the Fig. 15.

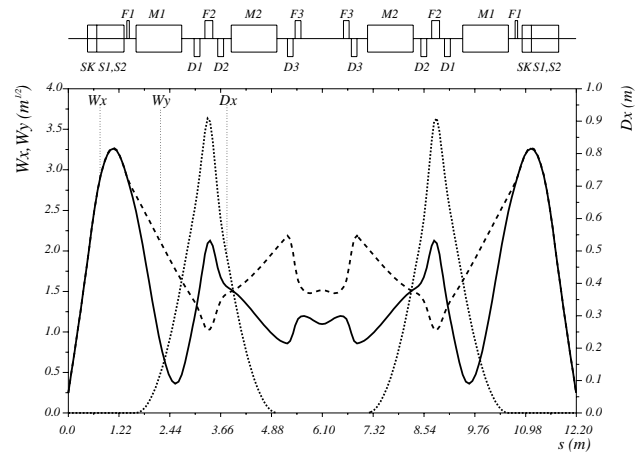


Figure 15: Half period lattice functions. $S = 0$ corresponds to IP

An essential advantage of the found optics is zero dispersion in the IRs, RF cavity, and injection straight sections.

The chosen optics has another very useful feature. Variation of the focusing strength of the solenoids changes β^*

and the beam emittance in inverse proportion, at fixed energy. Changing energy, we can squeeze β^* , conserving the maximum beam size at the solenoids, thus giving a possibility to tune optics for better performance. Apparently, this feature provides the luminosity scaling at lower energies approximately as γ^2 (instead of γ^4 for the option with fixed β^*).

The main parameters of the new collider are given in Table 4.

Table 4: Main parameters of the collider at E=900 MeV

Circumference, m	C	24.388
RF frequency, MHz	f_0	172.0
RF voltage, kV	V	100
RF harmonic number	q	14
Momentum compaction	α	0.036
Synchrotron tune	ν_s	0.003 ($\alpha = 0.04$)
Emittances, cm-rad	ε_x	$2.2 \cdot 10^{-5}$
	ε_z	$2.2 \cdot 10^{-5}$
Energy loss/turn, keV	ΔE_0	41.5
Dimensionless damping decrements	δ_z	$2.3 \cdot 10^{-5}$
	δ_x	$2.3 \cdot 10^{-5}$
	δ_s	$4.6 \cdot 10^{-5}$
Energy spread	σ_ε	$6.4 \cdot 10^{-4}$
β_x at IP, cm	β_x	6.3
β_z at IP, cm	β_z	6.3
Betatron tunes	ν_x, ν_z	4.1, 2.1
Particles/bunch	e^-, e^+	$1.0 \cdot 10^{11}$
Bunches/beam		1
Tune shifts	ξ_x, ξ_z	0.075, 0.075
Luminosity/IP, $\text{cm}^{-2} \cdot \text{s}^{-1}$	L_{max}	$1.0 \cdot 10^{32}$

2.8 Status of the Project

The designing of the main part of all the collider systems is finished. Manufacturing dipole magnets and quads is in progress and planned to be finished this year. Manufacturing and testing solenoids as the longest operation is planned to start this year and will continue the next year. The commissioning of the VEPP-2000 collider will start in the end of 2002.

3 STATUS OF THE PREINJECTOR COMPLEX VEPP-5

Preinjector complex VEPP-5 is being constructed for production and acceleration of electrons and positrons of up to 510 MeV [21]. Both kinds of particles would be accumulated in the damping ring and after achieving of needed intensity the beams will be transported alternatively to VEPP-3/VEPP-4M or to BEP/VEPP-2000 complexes. The scheme of the preinjector complex is shown in Fig. 16, where also the Φ -factory, 10 GeV linac and the beam line

to VEPP-5 collider are presented. But, due to lack of funding all these plans are suspended and, instead, a new beam line in the direction to VEPP-2000 collider is designed and will be built during coming two years. This will greatly improve the VEPP-2000 collider performance, because of significant increase of positron production rate.

The electron linac of preinjector VEPP-5 consists of two linacs, 300 MeV and 510 MeV. First accelerating structures of both linacs have an enhanced average acceleration rate of 25–30 MeV/m and other regular sections up to 17–20 MeV/m. During tests of the first 3-meter long accelerating structure an average rate of acceleration of the electron beam 35 MeV/m was achieved [22, 23]. Now the electron part of linac and one section of the positron linac are fully assembled. They are powered from the two SLAC-made 5045-type klystrons. One klystron feeds via the SLED pulse compression system three acceleration sections. The SLED input power is up to 60 MW with the pulse duration in $\Delta t \approx 3\mu\text{s}$, and its output power is up to ≈ 280 MW in $\Delta t \approx 0.5\mu\text{s}$. Now commissioning of the electron part of linac, as well as the positron conversion system are in progress.

Assembling of the damping ring and completion of the positron linac will be finished during the next year.

4 REFERENCES

- [1] V.Anashin et al., in Proc. EPAC'98, Stockholm, 1998, vol.1, p.400.
- [2] S.A.Nikitin, in Proc. of Intern. Workshop e+e- Factories'99, KEK, Japan, 1999, p.37.
- [3] E.Levichev, in Proc. HEACC-2000, Tsukuba, Japan, 2000, p..
- [4] V.E.Blinov et al, in Proc. PAC2001, Chicago, Illinois, USA, p..
- [5] A.A.Zolents, et al., Phys. Lett.,v.96B, No2, pp.214-216 (1981).
- [6] A.I.Gerasimov, et al., Necl. Inst. Meth. A305 (1991),p.25.
- [7] D.Shatilov, Part. Acc. 52, 65(1996).
- [8] V.Kiselev, E.Levichev, V.Sajaev, V.Smaluk, NIM A 406,pp.356-370, (1998).
- [9] V.A.Kiselev, S.A.Nikitin, I.Ya.Protopopov, in Proc. HEACC-98, Dubna, 1998, p.103.
- [10] V.Kiselev, E.Levichev, A.Naumenkov, in Proc. PAC2001, Chicago, Illinois, USA, p.
- [11] M.N.Achasov et al., Preprint BudkerINP 98-65, Novosibirsk, 1998.
- [12] R.R.Akhmetshin et al., Preprint BudkerINP 99-11, Novosibirsk, 1999.
- [13] P.M.Ivanov et al., in: Proc. 3rd Advanced ICFA Beam Dynamics Workshop, Novosibirsk, (1989), p. 26.
- [14] L.M.Barkov et al., in: Proc. 14th Int. Conf. High Energy Accelerators, Tsukuba (Japan), (1989), p.1385.
- [15] L.M.Barkov et al., in: Proc. of the IEEE Particle Accelerator Conf., San Francisco (1991), p.183

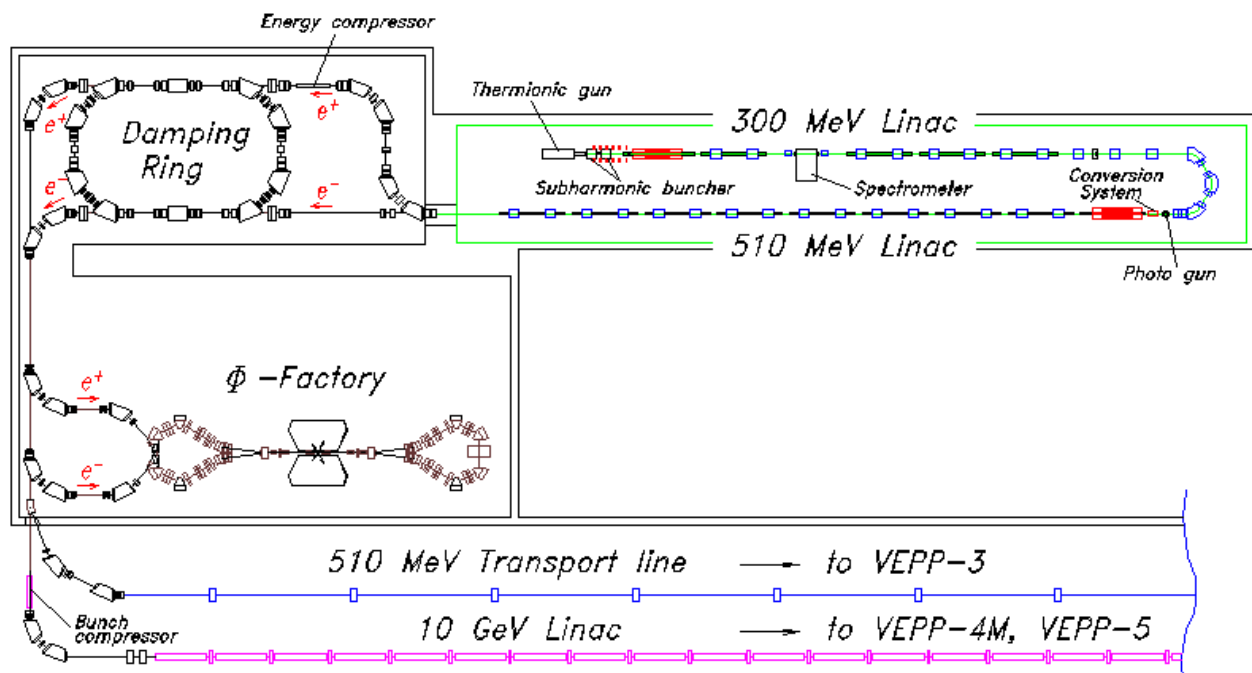


Figure 16: The scheme of VEPP5 Preinjector complex.

- [16] V.V. Danilov et al., "The Concept of Round Colliding Beams", in: *Proc. EPAC'96*, Barcelona (1996), p.1149.
- [17] A.N. Filippov et al., in: *Proc. 15th Int. Conf. High Energy Accelerators*, Hamburg (Germany), (1992), p.1145.
- [18] I. Nesterenko et al., in: *Proc. 1997 PAC*, Vancouver (Canada), (1997), p. 1762.
- [19] A.V. Otbojev and E.A. Perevedentsev, in: *Proc. 1999 PAC*, New York (1999).
- [20] V.V.Anashin et al., Preprint BudkerINP 84-114, Novosibirsk, 1984.
- [21] A.V. Alexandrov et. al., "Electron-positron preinjector of VEPP-5 complex". Proceedings of the XVIII International Linear Accelerator Conference., 26-30 August 1996, Geneva, Switzerland., CERN 96-07, 15 November 1996, Vol. 2, pp. 821-823.
- [22] V. Antropov et. al., "IREN test facility at JINR". Proceedings of the XVIII International Linear Accelerator Conference, 26-30 August 1996, Geneva, Switzerland, Vol. 2, pp. 505-508.
- [23] S.N. Dolya, W.I.Furman, V.V. Kobets, E.M. Lasiev, Yu.A. Metelkin, V.A. Shvets, A.P. Soumbaev, the VEPP-5 Team, "Linac LUE200. First testing results" (will be published).